G matrix stability in clinally diverging populations of an annual weed.

Georgia A. Henry[1*], John R. Stinchcombe[12]

[1] Department of Ecology & Evolutionary Biology, University of Toronto, Toronto, Ontario, Canada

[2] Koffler Scientific Reserve at Joker's Hill, University of Toronto, King City, Ontario, Canada

***Correspondence:** georgia.henry@mail.utoronto.ca

Abstract

How phenotypic and genetic divergence among populations is influenced by the genetic architecture of those traits, and how microevolutionary changes in turn affect the within-population patterns of genetic variation, are of major interest to evolutionary biology. Work on *Ipomoea hederacea*, an annual vine, has found genetic clines in the means of a suite of ecologically important traits, including flowering time, growth rate, seed mass, and corolla width. Here we investigate the genetic (co)variances of these clinally varying traits in two northern range-edge and two central populations of *Ipomoea hederacea* to evaluate the influence of the genetic architecture on divergence across the range. We find 1) limited evidence for clear differentiation between northern and southern populations in the structure of **G**, suggesting overall stability of **G** across the range despite mean trait divergence and 2) that the axes of greatest variation (g_{max}) were unaligned with the axis of greatest multivariate divergence. Together these results indicate the role of constraint on the divergence among populations across the range.

Keywords: G-matrix, quantitative genetics, multivariate evolution, clinal divergence, *Ipomoea hederacea*

Running title: Stable **G** across diverging populations

Introduction

A major goal in evolutionary biology is to understand the relationship between genetic variation within populations and phenotypic divergence between populations (Antonovics 1976, Endler 1977, Walsh & Blows 2009). Range edge populations provide an interesting setting in which to investigate this relationship. Populations existing on the margin of species' ranges are expected to have smaller population sizes (Brown et al. 1995), which are more susceptible to drift, and limited gene flow compared to more central populations (Sexton et al. 2009). Environmental gradients will often additionally create different selective pressures favouring phenotypic and genetic divergence. Here we examine the divergence and evolutionary potential of four populations of an annual plant, *Ipomoea hederacea*, sampled from the center and northern edge of the species' range with respect to five ecologically relevant traits.

The evolutionary response of a population undergoing selection is dependent not only on local selection, but on the underlying genetic architecture of the traits undergoing selection. The ability to adapt to the local environment depends on the amount of standing genetic variation as well as the genetic variance-covariance structure, represented as the **G** matrix (Antonovics 1976, Lande 1979, Lande & Arnold 1983, Falconer & Mackay 1996, Agrawal & Stinchcombe 2009). **G** is expected to shape evolutionary responses to selection as the relationships between traits lead to correlated responses selection (Lande 1979, Lande & Arnold 1983). Divergence among populations in response to local selection may thus be constrained or facilitated by the existing trait (co)variances. The multivariate trait combination with the greatest amount of genetic variation, dubbed the "genetic line of least resistance" by Schluter (1996) has been shown to influence macroevolutionary responses by deflecting the response to selection toward itself (Schluter 1996).

Whether **G** matrices themselves change along with trait means is not known. While **G** matrices exhibit some stability over evolutionary timescales (Schluter 1996, Arnold et al. 2008) we also expect population-level **G** matrices to undergo changes due to: bottlenecks (Roff 2000), inbreeding (Phillips et al. 2001), drift (Lande 1979, Jones et al. 2004), strong selection (with some genetic architectures) (Roff 2000), gene flow (Guillaume & Whitlock 2007), and genotype-by-environment interactions (Wood & Brodie 2015). The **G** matrices of populations located in ephemeral habitats or otherwise prone to extinction/colonization dynamics may reflect genetic drift because of small population sizes prior to extirpation (Lande 1992) and/or the effects of migration from limited or varied source populations due to colonization history (Whitlock & McCauley 1990), and may not be at equilibrium. Many of the biological forces that can affect **G**, in principle, could have contrasting effects between range-edge and central populations, making strong *a priori* predictions difficult. For instance, if range-edge populations are smaller and more subject to genetic drift, or under very strong selection because of novel conditions, we might predict less overall genetic variance, or different patterns of genetic covariance, in these populations. In contrast, if range-edge populations frequently experience swamping gene flow from the center of the range (Mayr 1954, Mayr 1963, Kirkpatrick & Barton 1997; Garcia-Ramos & Kirkpatrick 1997), their patterns of genetic covariance might show few differences compared to core populations. Consequently, whether and how range edge populations differ in **G** remains an empirical question.

Ipomoea hederacea, an annual plant which grows across the eastern U.S.A. from Pennsylvania to Florida, has latitudinal genetic clines in a variety of quantitative traits (Stock et al. 2014) and leaf shape (Bright 1998, Campitelli & Stinchcombe 2013), a Mendelian trait. These clines do not appear to be due to drift, but rather a response to selection, as no latitudinal patterns

in neutral loci have been found (Campitelli & Stinchcombe 2013; Campitelli & Stinchcombe 2014). Previous work by Stock and colleagues (2014) focused on among-population patterns and broad sampling found evidence of significant clinal divergence in three of the five traits (flowering time, anther-stigma distance and corolla width) while the remaining traits (seed mass, growth rate) had marginally significant divergence. These traits did not, however, exhibit a reduction of genetic variation in northern range edge populations compared to the central populations as was expected, suggesting there may still be sufficient variation for continued adaptation. Stock et al. (2014) estimated the axis of greatest multivariate divergence, that is the mean trait combination that is most different between populations of *I. hederacea* across latitudes, which we use here alongside more deeply sampled populations to compare within-population trait organization and among-population trait divergence.

Our research aims were: 1) to determine whether northern and southern populations differed in the overall heritability and genetic variance of the focal traits, 2) evaluate how genetic variation within populations was aligned relative to the axis of multivariate genetic divergence, and 3) assess population level divergence of the **G** matrices. To do so, we estimated trait heritability and the genetic variance-covariance matrices of four populations of *Ipomoea hederacea*; collected from the northern range edge (Pennsylvania and Maryland) and the core of the range (Hoffman and Ellerby, North Carolina). We expected the axis of trait divergence between populations to be biased toward the axis of greatest variation within populations, as this is the genetic line of least resistance (Schluter 1996).

Methods

Study species

Ipomoea hederacea is an annual weedy vine with an eastern North American distribution that spans Florida to Pennsylvania, USA (Bright 1998). While *I. hederacea* has existed in the present range for at least 150 years, its provenance is disputed, with some sources claiming it is native to its current range while others suggest it is introduced from the American tropics (Bright 1998, Campitelli & Stinchcombe 2014). *Ipomoea hederacea* is capable of mixed mating, but typically has a high selfing rate, with overall estimates ranging from 66-94% (Ennos 1981, Hull-Sanders et al. 2005, Campitelli & Stinchcombe 2014). Despite significant population structure, work using putatively neutral loci have found weak isolation-by-distance and no evidence of clines in neutral diversity (Campitelli & Stinchcombe 2013). There are, however, latitudinal clines in leaf shape (Bright & Rausher 2008, Campitelli & Stinchcombe 2013) and a suite of quantitative traits (Klingaman and Oliver 1996; Stock et al. 2014)

Propagation and trait measurements

We harvested seed from populations from the edge of agricultural fields in Pennsylvania (40.116611°, 76.398889°), Maryland (39.581861°, 77.816861°), Hoffman, North Carolina (35.074139°, 79.556694°) and Ellerby, North Carolina (35.091722°, 79.742722°). We sampled seed pods haphazardly from vines 1-2 m from one another, to reduce the chance of sampling twice from the same maternal plants, which were the founders of the matrilines we used in our experiments. We grew one seed from 50 randomly chosen matrilines per population in a common greenhouse environment and allowed these individuals to self-fertilize. One death prior to seed set resulted in 49 matrilines in Ellerby, NC. We harvested selfed seeds from each

maternal plant and grew approximately 11 focal individuals (range: 2-11, mean = 10.7) from each line for this study, resulting in a total sample of 2,133 plants. While our use of selfed progeny precludes estimating additive genetic variance, selection acts on the broad sense variation rather than just the additive components of variation in mainly selfing species (Roughgarden 1979), making this design appropriate for *I. hederacea*.

We grew plants in cone-tainers (Stuewe & Sons, Oregon, USA) filled with Pro-Mix soil in a glasshouse at the University of Toronto from April-October 2018. All plants were fertilized with a weak 10-52-10 fertilizer solution every 2 weeks. Day length was initially 16 hours at 28°C, changed to 12 hours at 25°C on day 32, and 8 hours at 22°C on day 38 to promote flowering.

Trait measurements followed Stock et al. (2014). Prior to planting, we weighed each seed and recorded individual mass. We counted leaves at 17 days after planting and again on the 26th or 27th day of planting; we estimated growth rate as the difference in leaf counts divided by the number of days, and as such it is in units of new leaves/day. We measured corolla width and anther-stigma distance on the first flower of each individual using calipers. We measured the distance from the lowest and highest anthers to the stigma and calculated the mean of the absolute distance to characterize anther-stigma distance.

Data preparation

Four of the five focal traits, (seed mass, early growth rate, corolla width and anther-stigma distance) were standardized to mean = 0 and standard deviation = 1 using the grand mean and standard deviation across populations to allow for meaningful comparison of differences (Hine et al. 2009, Hansen & Houle 2008). We elected to use this standardization to eliminate differences in the scale and units of our traits (e.g., anther stigma distance in mm, growth rate in

leaves per day, and flowering time in days) and because mean standardization can be difficult to apply to traits like flowering time, which have an arbitrary rather than natural zero (Hansen & Houle 2008, Houle et al. 2011). As the glasshouse was exposed to ambient light, the change in artificial light used to induce flowering was largely overwhelmed by the natural photoperiod. A change from lengthening to shortening days interrupted the flowering schedule. For this reason we transformed the number of days until the first flower using ordered quantile normalization (ORQ), which preserves the order of flowering but results in a gaussian distribution (Peterson and Cavanaugh 2019). The ORQ normalization results in a distribution centered on zero with a standard deviation of one, which is the same scale as all other traits.

Univariate analysis

To determine broad sense heritabilities of the traits we fit Bayesian generalized linear mixed-effect models for each trait in each population separately. We estimated the models using MCMCglmm in R (Hadfield 2010) using the mixed model,

$$y = \mathbf{X\beta} + \mathbf{Z}_1\mathbf{u}_1 + \mathbf{Z}_2\mathbf{u}_2 + \mathbf{e} \qquad \textbf{(1)}$$

For each trait, y, we ran a separate model. In (1), $\mathbf{X}$, $\mathbf{Z}_1$ and $\mathbf{Z}_2$ represent design matrices for the fixed effect of population, and random effects of matriline and greenhouse block, respectively. $\boldsymbol{\beta}$ and $\mathbf{u}$ are vectors of the related parameters. We included the environmental block to control for the effect of microenvironmental differences within the glasshouse. For seed mass, we used the greenhouse block of the maternal plant. The residual error is represented by **e.**

We tested six priors and summed the Deviance Information Criteria for each of the five univariate models. We used the prior with the lowest summed DIC score, although due to the amount of data in the model the prior choice was not very influential. The effective size of the samples was greater than 85% of the total number of samples and the autocorrelation was below

0.05 for all parameters (Hadfield 2010). To evaluate whether there was meaningful broad sense heritability, we ran models within each population with and without the matriline variable and compared DIC values, per Puentes et al. (2016). We considered models where the matriline reduced the DIC score >2 to have a "significant" genetic component and thus H2 was significant. We constructed comparable models for validation, using REML, which are presented in the Supplemental Material. Heritability estimates were similar, with the greatest difference in Heritability of 5.2%, and an average absolute difference of 1.7%.The 95% Highest Posterior Density (HPD) intervals from Bayesian models overlapped REML heritability estimates in all cases, and as such Bayesian estimates are presented in the main text.

Multivariate Analyses

We estimated the total genetic variance-covariance matrices separately for each population using Bayesian generalized linear mixed-effect models through MCMCglmm in R (Hadfield 2010). We again used the mixed model,

$$\mathbf{y} = \mathbf{X\beta} + \mathbf{Z}_1\mathbf{u}_1 + \mathbf{Z}_2\mathbf{u}_2 + \mathbf{e} \qquad \textbf{(3)}$$

where $\mathbf{X}$, $\mathbf{Z}_1$ and $\mathbf{Z}_2$ represent design matrices for the vectors of trait means ($\boldsymbol{\beta}$)**,** the total genetic effects ($\mathbf{u}_1$) and the Greenhouse Block effects ($\mathbf{u}_2$). The residual error is represented by the term $\mathbf{e}$.

We used weakly informative inverse-Wishart priors for estimating the variance and covariances where the distribution was described by the variance (V) and the belief parameter (nu) and the default prior for the fixed effect estimates, $N(0,10^8)$. We tested a variety of priors to determine the robustness of estimates and selected the model with the best fitting prior, determined by the lowest average Deviation Information Criteria score to use for our analyses (see Supplementary Materials). The final prior for the residual variance was given by a diagonal

matrix of 1's with the degree of belief slightly above *n*-1, for *n* traits (V=diag(5), nu = 4.001). The best prior for the random effects was a matrix of ⅓ the phenotypic variance-covariance matrix and a belief parameter slightly above *n*-1 (V = (**P**/3)*10, nu=4.001, where **P** is the phenotypic covariance matrix). All the response variables in the model were multiplied by a factor of 10, which improves the estimation of small variances (and is subsequently factored out of the genetic variance-covariance matrix). To account for this factor of 10 in the response variables, the Phenotypic variance-covariance matrix (**P**) was also multiplied by a factor of 10 in the priors.

We ran full models for 5,005,000 iterations, with a burn in of 5,000 and a thinning interval of 1,000, resulting in 5000 iterations sampled from the posterior distribution. The effective size of the samples was greater than 85% of the total number of samples and the autocorrelation was below 0.05 for all parameters (Hadfield 2010).

Null Models

For some analyses, a null model was necessary, as MCMC methods can only estimate variance greater than zero (matrices must be positive definite). We constructed randomized **G** matrices where the values only reflected sampling error as a point of comparison to our actual estimates. Following Walter et al. (2018) and McGoey and Stinchcombe (2021), we randomly assigned individuals to matrilines within populations, without replacement, resulting in **G** matrices that are only due to sampling error, as any phenotypic similarity among individuals is only due to random sampling, rather than true genetic ancestry. Our design includes significant fixed effects, which Morrissey et al. (2019) note will make these null distributions larger than they should be, which should make our approach conservative. We also note that because each randomized **G** matrix only reflects sampling variation, the expectation of a large number of **G**

matrix comparisons should be near 0 (as each population only reflects sampling variation), but the distribution of these comparisons reflects the range of potential outcomes one can obtain if each **G** only reflects sampling, making it a sensible null model for comparisons. The within-population randomization approach also allows us to compare whether each estimated **G** differs from expectations due to sampling (Sztepanacz and Blows 2017).

We fed each randomized "population" into the same models as the observed data, run for 20,000 iterations with a burn in of 5,000 and a thinning interval of 100. We iterated the randomization and model estimates 1000 times. We combined the final posterior sample of each of the randomized models within populations to be used as a composite posterior. We assessed chains visually for stability and with Gelman and Rubin convergence diagnostic criteria.

G matrix comparisons

We used several metrics to compare G matrices, each of which has different strengths and weaknesses (Krzanowski 1979, Kirkpatrick 2009, Hine et al 2009, Aguirre et al. 2014, Puentes et al. 2016, Walter et al. 2018, Teplitsky et al. 2014). In general, our goal was to use a variety of metrics to compare G matrix size, shape, concordance between patterns of genetic variance and clinal divergence, and similarity in the responses to selection that each G matrix would produce.

G matrix dimensionality

We calculated the trace of the **G** matrices to determine the total amount of genetic variance in each population. We then evaluated the overall strength of the covariance by calculating the effective number of dimensions, n_D (Kirkpatrick 2009), which is the sum of the eigenvalues divided by the leading eigenvalue. The effective number of dimensions ranges

between 1, which would indicate that all of the genetic variance was in a single direction in multivariate space, and the number of traits, which would indicate that the traits are equally genetically variable and uncorrelated.

Genetic variation in the direction of maximum clinal divergence

To evaluate the alignment between the axis of greatest genetic variation (g_{max}) of each population, and between g_{max} and the vector of greatest multivariate divergence ($Cline_{max}$ from Stock et al. 2014) we calculated the correlation coefficient between these vectors. We used random unit vectors as a null comparison. We note that Stock et al. (2014) used and presented results from mean-standardized data; we re-analyzed their data to estimate the vector of greatest clinal divergence using standard deviation standardized data, to match our use of standard deviation-standardized data from the greenhouse experiment.

We projected the vector of maximum clinal divergence through each **G** matrix (using $b^T\mathbf{G}b$, where b is the vector of clinal divergence; see Lin and Allaire 1977) to calculate the genetic variance in direction of clinal divergence. To estimate the proportion of genetic variance along the direction of maximum clinal divergence, we estimate $b^TGb/\boldsymbol{\lambda}_1$, where $\boldsymbol{\lambda}_1$ is the first eigenvalue of **G**, representing the vector of maximum genetic variance in each population. Given that the **G** matrices had different shapes, the maximum amount of genetic variation in any direction differed between the populations. To allow for fair comparison, we standardized by the proportion of variance associated with g_{max}, the first eigenvector of **G**.

Random skewers

We performed a random skewers analysis (Cheverud & Marriog 2007, Aguirre et al. 2014) following Aguirre et al. 2014. Briefly, 1000 randomly generated normal vectors were

projected through each population's **G**. We compared the response from each projection between populations to determine which random vectors which produced response differences. We then calculate the variance-covariance matrix of the skewers which result in response differences between populations and perform eigenanalysis to generate the **R** matrix. The **R** matrix describes the trait space where differences in the response to skewers exist between populations, with the first eigenvector describing the axis with the greatest differences between populations.

Krzanowski's subspace analysis

Krzanowski's subspace analysis provides a method of evaluating the similarity in geometry of multiple variance-covariance matrices. The approach works by examining whether the subspaces containing most of the genetic variation (e.g., the leading PCs) in each population are shared, or in common. We first determine the shared space (**H**) of all populations, from a subset of the leading PCs (eigenvectors) of each population, using:

$$\mathbf{H} = \sum_{t=1}^{p} \boldsymbol{A}_t \boldsymbol{A}_t^T \qquad \textbf{(4)}$$

where superscript T indicates transposition, and a subset *t* of PCs of each **G** matrix are included in **A**, and summation is to *p* populations (*p* = 4 in our case; Krzanowski 1979; Aguirre et al. 2014). As per Aguirre et al. 2014, the number of eigenvectors used for each population were those which explained >90% of the total variation to account for differences in the shape of the population **G** matrices. The eigenvalues of **H** can range from 0 to *p*, which indicates common sub-spaces to the matrices being compared (i.e., the leading PCs describe similar directions of multivariate space). If the eigenvalues of H are less than *p* (4 in our case), this indicates that genetic variation described by that eigenvector differs among the populations. To evaluate which populations are most similar we determine the smallest angle between the mean posterior subspace of each population and the mean shared subspace **H**, as per Aguirre et al. 2014.

Tensor analysis

Differences between matrices can be evaluated by calculating the 4th order covariance tensor, describing the variances and covariances between matrices (Hine et al. 2009). We used the 4th Order Genetic Covariance Tensor analysis developed by Hine et al. (2009), and outlined by Aguirre et al. (2014), and Walter et al. (2018). We refer interested readers to these papers for full details (especially Fig. 2 of Walter et al. 2018), and only provide a brief overview here. The fourth order tensor of the matrices describes the variance and covariances among the population **G** matrices. The tensor can be represented as a symmetric (n(n+1)/2) matrix (**S**) (Basser & Pajevic 2007), with elements describing the variances and covariances of genetic variances and covariances in the four populations. The matrix **S** can then be subject to eigenanalysis, where eigenvalues and eigentensors describe how the **G** matrices vary. Eigentensors with larger eigenvalues (which explain a larger percentage of variance) describe dimensions of greater variation in the **G** matrices; the eigentensors can themselves be subjected eigenanalysis, to determine the linear combination of traits (eigenvectors) that lead to the difference in **G** matrices captured by the eigentensors. The covariance tensor analysis can thus be used to evaluate axes of differences among the genetic variance-covariance structure of the populations.

Results

Univariate Analyses

We estimated broad-sense heritability of each trait within populations using a Bayesian model (Table S1, Figure S1), and confirmed results with REML (Table S2) as described above. All traits had heritability greater than zero in at least 3 of the 4 populations (Table S1). The Pennsylvania population lacked significant heritability for anther-stigma distance (Table S1).

The mean of all the heritability estimates was 0.213 (ranging from 0.011 to 0.535). There was no significant difference between northern and southern populations, although northern populations tended to have lower heritability estimates than southern populations (Table S1).

G matrix dimensionality

We present population **G** matrices, 95% HPD intervals, and null expectations due to sampling variation in the Supplemental Material (Table S3, Table S4), and in the main text focus on comparisons of the matrices. Our **G** matrices all contain variances with HPD intervals that do not overlap the 95% HPD intervals of the null **G** matrices, although some traits in some populations did have overlapping 95% HPD intervals indicating that the variation may be very small (Table S3). Two of the traits, corolla width and anther-stigma distance, have variation indistinguishable from sampling variation in all populations except Hoffman (Table S3); we nonetheless retained these traits in our analyses to allow comparisons of **G** properties to divergence in trait means, which requires these traits. All populations have an effective number of dimensions considerably less than the number of traits measured (Table 1), indicating that the genetic covariance is important in all cases. There were no population level differences, as the 95% HPD intervals of all populations overlapped one another. The northern populations (Pennsylvania and Maryland) had slightly smaller effective dimensions indicating overall greater correlation among traits, but the 95% HPD intervals overlapped.

We found that Hoffman, NC had significantly greater total genetic variation than all other populations, which we estimated as the trace of the **G** matrices. Hoffman had approximately twice the amount of genetic variation than populations from Ellerby, NC and Maryland, and three times that of Pennsylvania. The 95% HPD intervals of Hoffman did not overlap with those of any other population.

Table 1: Effective number of dimensions (N dimensions) for each population **G** matrix and the total amount of genetic variation in each population, estimated as the trace of **G**. Low and high values demarcate the 95% highest posterior density interval (HPD).

Population	N dimensions	Lower HPD	Upper HPD	Trace of G	Lower HPD	Upper HPD
Pennsylvania	1.887	1.440	2.371	0.518	0.367	0.685
Maryland	1.887	1.454	2.378	0.764	0.545	1.006
Hoffman, NC	2.068	1.579	2.608	1.615	1.208	2.054
Ellerby, NC	2.007	1.535	2.509	0.886	0.644	1.176

Genetic variation in the direction of maximum clinal divergence

Overall the proportion of genetic variation in the direction of maximum clinal divergence was small, roughly on par with the third eigenvalues of each population, and there were no significant differences between any populations (Table 2). To fairly compare between populations, which differ in their total amount of genetic variation (Table 1) and the variation along g_{max} (Table S5), we standardized the genetic variance in the direction of clinal divergence by the genetic variance associated with g_{max}, so the values are relative to the linear combination of traits with the maximum possible genetic variance in each population. The standardized projections of the northern populations were slightly larger than the southern populations, but there were no significant differences between them. In general, genetic variance in the direction of clinal variation was ~25-50% of the genetic variance associated with g_{max}.

Table 2: Genetic variance in the direction of maximum clinal divergence for each population. In the standardized column (Variance (std)), the variances are standardized by the eigenvalue of the leading eigenvector of each population, to express this relative to the direction of greatest genetic variation. Lower and higher HPD values demarcate the 95% highest posterior density interval.

Population	Variance	Lower HPD	Higher HPD	Variance (std)	Lower HPD	Higher HPD
Pennsylvania	0.102	0.047	0.176	0.371	0.174	0.602
Maryland	0.157	0.076	0.252	0.383	0.203	0.570
Hoffman, NC	0.204	0.092	0.325	0.266	0.104	0.456
Ellerby, NC	0.227	0.106	0.361	0.512	0.266	0.782

The correlation between gmax from each of the G matrices and direction of maximum clinal divergence is low and not significantly different from the expected correlation between gmax and a random vector (Figure 1). Although we might expect the direction of maximum clinal divergence to be aligned with directions of genetic variation, this does not appear to be the case for any population. The correlation between PC2 through PC5 of the population G matrices and direction of maximum clinal divergence followed the same pattern (Figure S2).

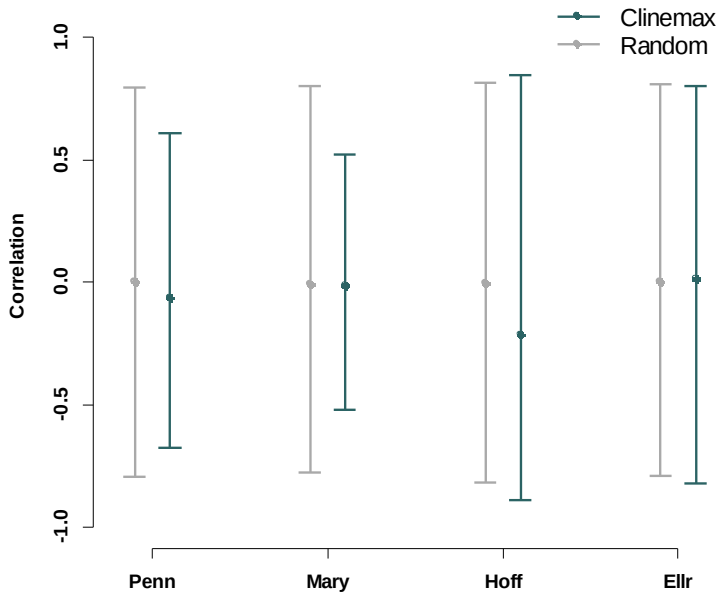

Figure 1: The correlation between the g_{max} of each population **G** matrices and the vector of greatest multivariate clinal divergence (Observed, in blue) compared to the correlation between the g_{max} of each population **G** matrices and randomized vectors (Randomized, in, in gray). Error bars represent the 95% HPD intervals. "Penn" is Pennsylvania, "Mary" is Maryland, "Hoff" is Hoffman, NC and "Ellr" is Ellerby, NC.

Random skewers

The majority of random vectors produced some difference in response between populations, with 588 of 1000 resulting in responses where at least one pairwise comparison had 95% HPD intervals which did not overlap. Following Aguirre et al. (2014), we took this subset of vectors which resulted in response differences and created a variance-covariance matrix of the vectors. We then performed eigenanalysis to evaluate the trait space which describes differences

between populations. The highest trait loading of the first eigenvector is corolla width, followed by seed mass and flowering time (table 3). These differences in response are largely attributable to Hoffman, NC. Projecting the eigenvectors of the **R** matrix through each population's **G** matrix, we found that Hoffman had significantly more genetic variation along this eigenvector than the other three populations (Figure 2). In other words, the response difference we detected with random skewers appears to be due to the Hoffman population having more genetic variation for a linear combination of traits made up primarily of seed mass and corolla width, with lesser but nearly equal contributions of growth rate and anther stigma distance, than the other three populations.

Table 3: Eigenanalysis of the **R** matrix from the Random Skewers analysis which resulted in difference in response when projected through populations. The **R** matrix summarized the trait combinations which resulted in differences to the projected response. Each eigenvector (RSe1 through RSe5) describes an independent combination of traits which capture differences among populations. The eigenvalues describe the proportion of variation of each eigenvectors within **R**, larger values indicate more of the variation in the skewers are explained.

Trait	**RSe1**	**RSe2**	**RSe3**	**RSe4**	**RSe5**
Seed mass	-0.579	-0.147	0.211	-0.404	0.660
Growth	-0.262	-0.131	0.776	-0.075	-0.554
Flow time	-0.337	-0.587	-0.106	0.727	0.052
Corolla	-0.622	0.124	-0.556	-0.234	-0.483
AS dist.	-0.309	0.776	0.180	0.498	0.149
Eigenvalues	0.303	0.253	0.232	0.115	0.095

The second and third eigenvalues of **R** are of similar magnitude, and when projected through the **G** matrices, reveal similar patterns. The second axis of **R** captures trait combinations with opposing and larger values for anther-stigma distance and flowering time (Table 2); we observe that Hoffman had more genetic variation for this combination of traits than the Maryland and Pennsylvania populations. The third axis of **R** reflects trait combinations with opposing and larger values for corolla width and growth rate, and Hoffman had more variation for that combination of traits than the Maryland population. Collectively, these data indicate that the

differences in the **G** matrices detected by random skewers were primarily driven by the Hoffman population, and it having more variation linear combinations of traits involving all of the traits measured (*RSe1*: corolla width and seed mass in concert; *RSe2*: flowering time and anther stigma distance in opposition; *RSe3*: corolla width and growth rate in opposition). The Hoffman population also had the highest heritability for all of the measured traits (Table S1), the largest effective number of dimensions (Table 1), and the largest trace of **G** (Table 1).

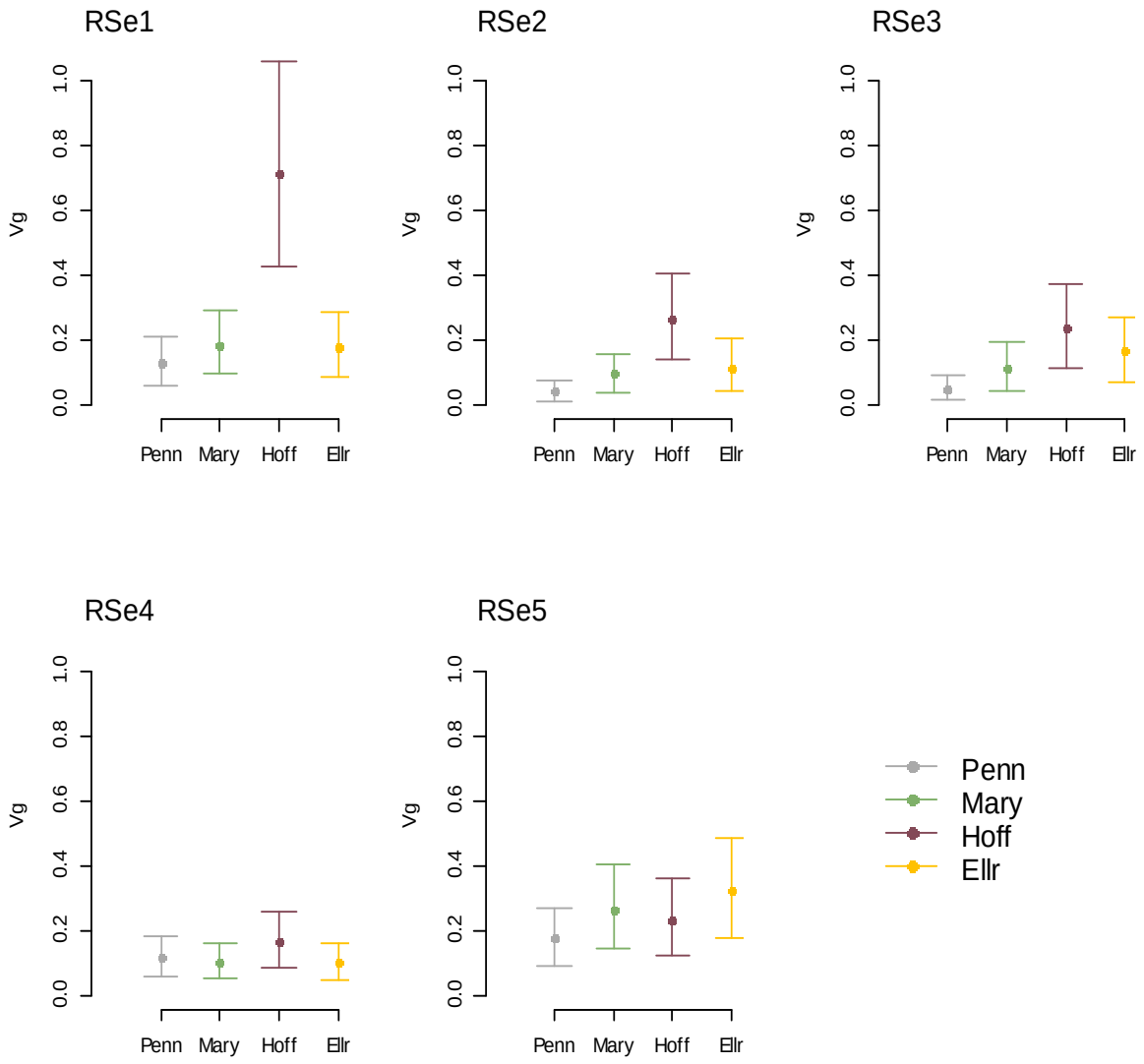

Figure 2: Genetic variance (Vg) in the direction of each eigenvector of the **R** matrix, where the **R** matrix is composed of vectors which resulted in response differences between populations.

Krzanowski's subspace analysis

To construct **H**, the shared subspace, we used the number of eigenvectors which explained at least 90% of the variation in each population. The first three eigenvectors of each population satisfied this condition. Lambda, which ranges from 1 to 4, approaches 4 in the first two eigenvectors of **H** (Table 4, Figure 4). A lambda value nearing 4 means the populations all

contain the variation sufficient to recreate the shared trait space. Thus, the populations contain considerable shared trait space in the first two dimensions of **H**. The third eigenvalue is lower, but is similar to the randomized comparison (Figure 4). Overall there is no evidence of divergence among populations in the shared subspace.

Table 4: Eigenvalues (lambda) for each eigenvector of the shared subspace **H** with the 95% HPD intervals. A value of 4 would indicate that all the populations have the variation in their subspaces required to recreate the respective eigenvalue of **H**, lower values indicate that populations do not and thus lack similarity.

Eigenvector	Lambda	Lower HPD	Higher HPD
h1	3.840866	3.655673	3.978588
h2	3.04281	2.477581	3.798831
h3	2.284866	1.538301	3.009639

To evaluate any population level divergence from the shared subspace we can calculate the angle between the axes of **H** and the subspaces of the populations ($\mathbf{A}_t\mathbf{A}_t^T$), which capture at least 90% of the genetic variation in each population. Larger angles indicate that population differs in some manner along that axis of shared subspace. The first three eigenvectors of Pennsylvania, Hoffman and Ellerby, and Maryland were used to generate the shared subspace. Overall the angles between **H** and the population subspaces are similar and small with increasing uncertainty for higher eigenvectors (Figure S3), meaning differences between the populations and the shared trait subspace are minimal.

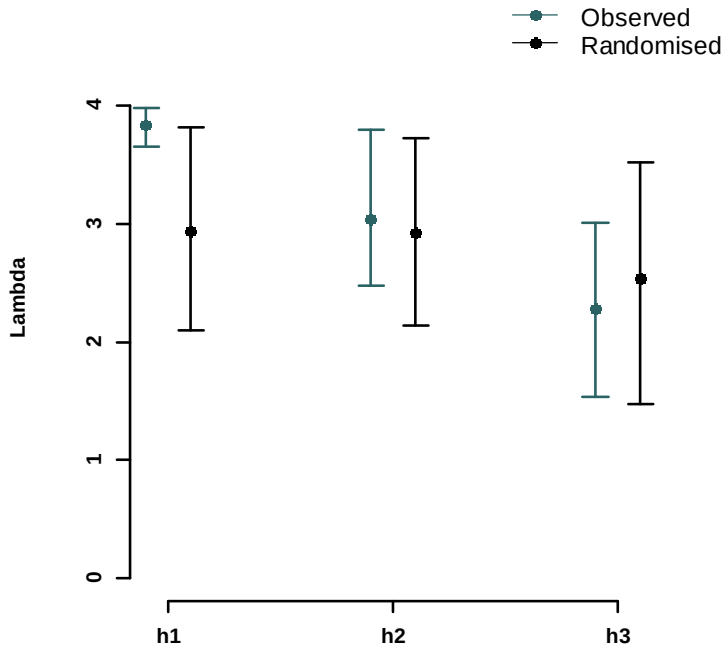

Figure 3: Eigenvalues (lambda) for each eigenvector of the shared subspace **H**, (where h > min k). Higher values of lambda indicate greater similarity of population subspaces.

Covariance tensor analysis

We calculated the fourth order covariance tensor for the population **G** matrices to assess areas of divergence between the populations. We used the randomized **G** matrices, which represent sampling variation within populations, as a null contrast to assess significance. For the observed **G** matrices, we estimated three non-zero eigentensors for tensor **S**. Of these three eigentensors, the first two have eigenvalues significantly different from a null expectation based on sampling variation creating each **G** matrix independently (Table S6, Figure 6).

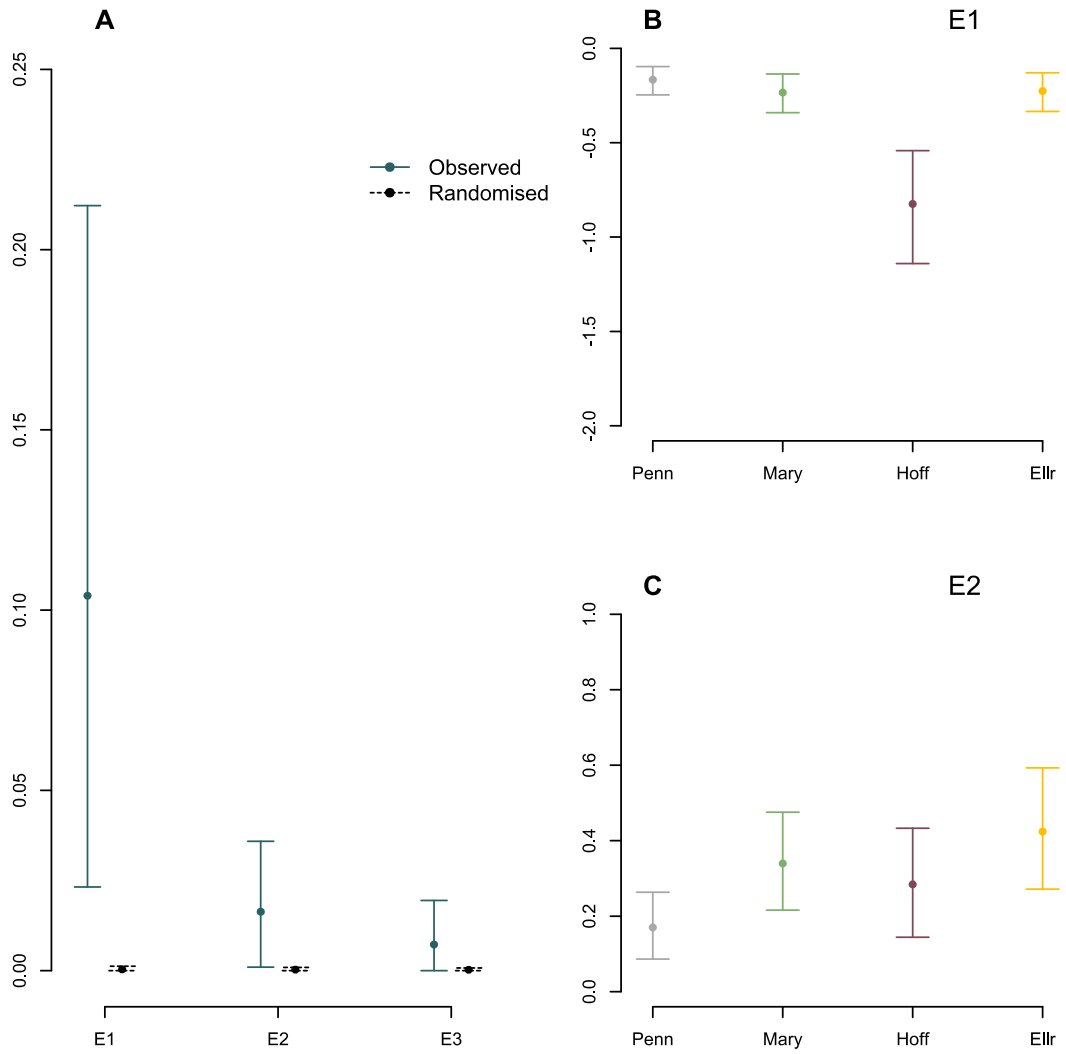

Figure 4: A) Eigenvalues (**α**) for each non-zero eigentensor from the observed and randomized **G** matrices. Note that the upper and lower bounds of the randomized data, reflecting only sampling variation, are small and hard to distinguish on the figure. B) Coordinates of each population in the first non-zero eigentensor of **S**, E1. C) Coordinates of each population in the second non-zero eigentensor of **S,** E2.

To determine the contributions of each population to the eigentensor, we estimated the coordinates of the populations within each eigentensor. The greater the absolute value of the coordinate the greater the contribution a population has. In the first eigentensor (E1, which explains 81.5% of the variation across all non-zero eigentensors), Hoffman again stands out from the other populations and has the greatest contribution. Thus the first eigentensor, which

describes the greatest amount of variation among the population **G** matrices, is largely driven by differences between Hoffman, NC and all the other populations. In contrast, Ellerby, NC has the largest coordinate value in the second eigentensor (E2), which explains 12.8% of the variation among **G** matrices.

Eigenanalysis of the eigentensors reveals that the first eigenvector of E1, (*e11*) which explains 47.6% of overall variation (58.4% of variation within E1), is most heavily weighted by seed mass and corolla width (similar to *e1* of the **R** matrix, as analyzed by Random Skewers), with all trait loadings being of the same sign (Table 5). The first eigenvector of E2 *(e21)*, which explains 5.9% of overall variation among populations (45.9% of variation in E2), describes a dimension most heavily weighted by the seed mass and growth rate of opposing signs (Table 5). Thus these two eigentensors describe population differences in the relationship between seed mass and other traits, especially with respect to the southern populations.

Table 5: Eigenvectors of each non-zero eigentensor of observed **S**. The variance explained by each eigentensor of **S** is given, along with the eigenvalues of each eigentensor in the direction of each eigenvector. These values describe the contribution of the independent trait combinations described by the eigentensors. The proportion of variance is the proportion of variance of the eigentensors explained by each eigenvector. The trait loadings for eigenvalues of each of the three eigentensor are given, along with the eigenvalue of the eigentensors.

Eigenvector	σ of E_x	Eigenvalue	Prop. of σ	Seed mass	Growth	Flow time	Corolla	AS dist.
e1.1	0.815	-0.912	0.584	-0.611	-0.152	-0.323	-0.612	-0.354
e1.2		-0.317	0.203	0.044	0.379	-0.674	-0.140	0.617
e1.3		-0.254	0.163	0.568	0.519	-0.088	-0.342	-0.532
e1.4		0.049	0.031	0.542	-0.751	-0.312	-0.210	0.034
e1.5		-0.031	0.020	0.089	0.031	0.581	-0.667	0.457
e2.1	0.128	0.830	0.459	0.696	-0.639	-0.284	-0.097	0.134
e2.2		0.406	0.225	0.631	0.621	0.247	-0.387	-0.077
e2.3		-0.329	0.182	0.070	-0.288	0.896	0.167	0.286
e2.4		0.189	0.105	-0.253	0.019	-0.104	-0.596	0.754
e2.5		-0.054	0.030	-0.222	-0.352	0.212	-0.676	-0.571
e3.1	0.057	0.651	0.347	-0.005	0.811	0.441	0.315	0.220
e3.2		-0.640	0.341	0.946	-0.089	0.000	0.300	-0.081
e3.3		0.362	0.193	-0.228	-0.349	0.567	0.473	-0.530
e3.4		0.184	0.098	-0.116	-0.415	0.047	0.455	0.778
e3.5		-0.041	0.022	-0.197	0.202	-0.695	0.617	-0.240

We next projected these eigenvectors through the population **G** matrices, as we did for the random skewers, to assess how much variation each population has along these axes. Not unexpectedly, Hoffman, NC has significantly greater genetic variation along the first and second eigenvector of E1 (Figure 5). Hoffman again has greater variation than the other population along the first eigenvector of E2, although the HPD intervals overlap for Ellerby, NC, the other southern population. The second eigenvector of E2 similarly has overlapping 95% HPD intervals for all populations but the southern populations have slightly more genetic variation in this direction than the northern populations.

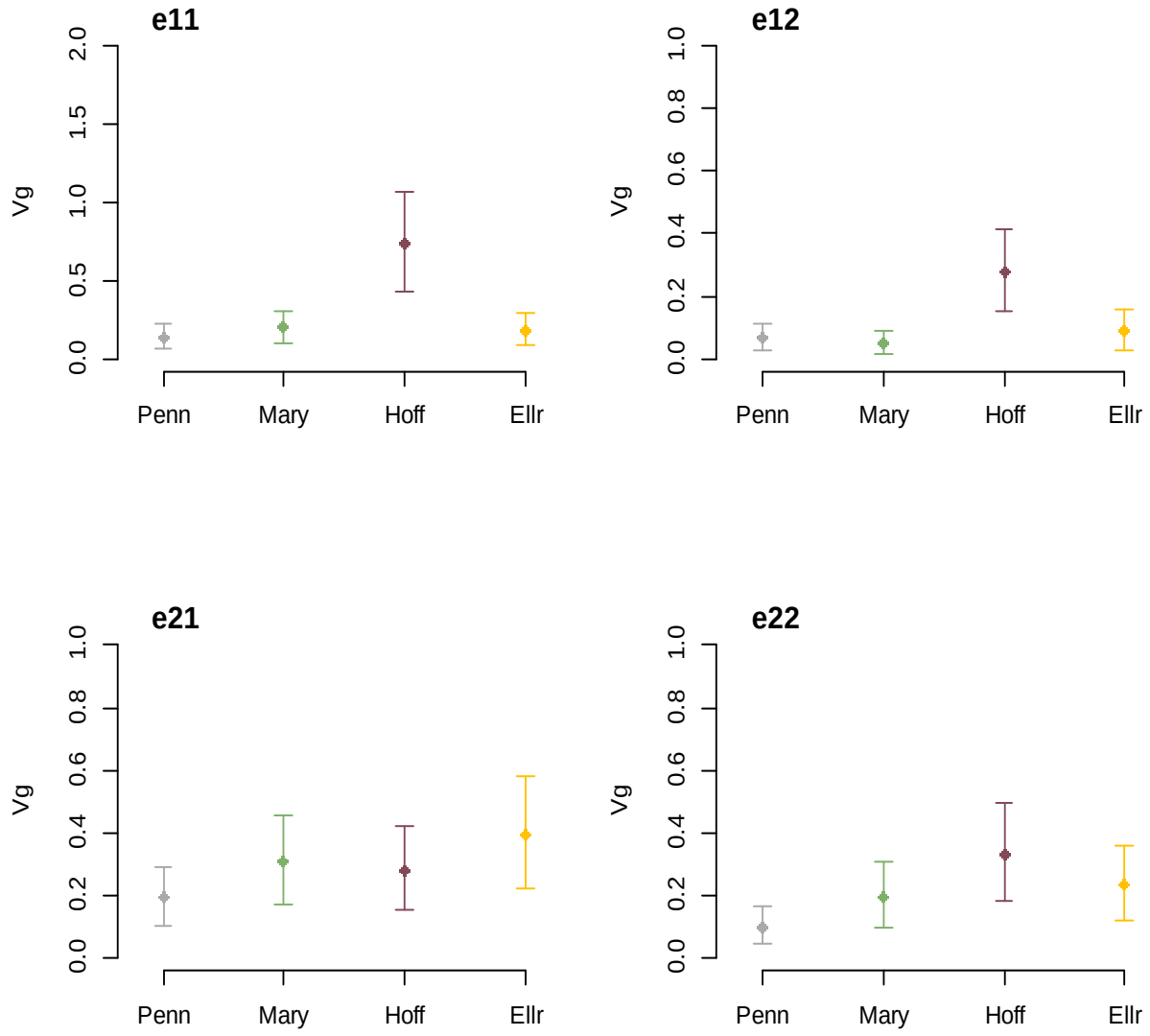

Figure 5: Genetic variation in the direction of eigenvectors of the fourth-order covariance tensor **S**. e11 is the first eigenvector of the first eigentensor, e12 is the second eigenvector of the first eigentensor, e21 is the first eigenvector of the second eigentensor, e22 is the second eigenvector of the second eigentensor. The vectors were projected through each of the **G** matrices to determine the amount of genetic variation that exists in that dimension.

Similarity between skewers and tensors

Given the similarities between the first eigenvector of E1 of **S** and the results from the random skewers **R** matrix projection we calculated the correlation between the two vectors and

found that they are almost perfectly correlated (corr = 0.992). This congruence between two vectors of differentiation calculated with entirely different methods provides additional support for this axis describing considerable differences among populations.

Discussion

Understanding patterns of genetic variation within populations, and how they relate to phenotypic differentiation among them, is a central goal in evolutionary biology. Our analyses of genetic (co)variance matrices and divergence of four natural populations of *Ipomoea hederacea* point to three main results. First, we found that overall correlations between traits are important, reducing the dimensionality of **G** in all four populations, and thus the potential for independent phenotypic trait evolution. While northern populations tended to have greater dimensionality reduction, reduced overall genetic variation, and lower trait heritabilities, the posterior distributions of these parameters overlapped for northern and southern populations. Second, contrary to our expectations, the axis of greatest multivariate clinal divergence was not aligned with the axis of greatest variation in any population, suggesting a role for constraint and selection in the divergence of these populations. Third, we found that the populations tended to have similar patterns of **G** matrix structure and inhabit the same trait space, with the notable exception of one population. Below, we discuss these results in light of how genetic constraints and reduced dimensionality of **G** influence phenotypic divergence, and divergence in **G** these populations.

Evolutionary potential and divergence of G

Our study of **G** within these four populations allows both an evaluation of the evolutionary potential within each population, and the divergence (or lack thereof) of **G** itself

between range-edge adjacent populations and the central core. Using a variety of approaches, including estimating the effective number of dimensions, the trace of **G**, and a handful of methods for comparing **G** among populations (Krzanowski's subspace, covariance tensors, random skewers), we found a consistent pattern of results. These populations all appear to be of reduced rank, have similar amounts of total genetic variance, and there do not appear to be appreciable differences between range-edge populations and core populations in the structure, size, or shape of **G**.

We first assessed the general structure of the populations and found that all four have an effective number of dimensions around two, appreciably less than the number of traits evaluated. Our results indicate that while we might observe and measure these traits separately (and can detect significant genetic variation in them, individually), the patterns of genetic covariances in them mean that there are effectively fewer independent traits. Reduced effective dimensionality suggests the importance of these trait correlations in all of the populations. Much of the multidimensional trait space lacks detectable genetic variation (Kirkpatrick 2009), and populations are likely to be evolutionarily constrained if selection were favoring trait combinations completely lacking variation (see Kingsolver et al. 2015). While there were no differences in the effective number of dimensions, there were differences in the amount of total genetic variation among populations. Hoffman, NC, one of the southern populations, possessed significantly greater variation than all other populations. While the second southern population, Ellerby, NC did have slightly higher genetic variation, the HPD intervals overlap those of the other populations. Similarly, trait heritabilities tended to be higher in southern populations (Table S1), albeit again with overlapping HPD intervals. As such, it appears that the Hoffman population is distinct from the rest, rather than southern populations on the whole differing from

northern populations. Two of the traits, corolla width and anther-stigma distance, had very small variances indistinguishable from sampling variance in three of the populations (Hoffman again being the exception). The lack of variation in in these traits in **G** make observing differences among populations impossible with respect to corolla width and anther-stigma distance. We retained these traits in our **G** matrices so as to allow for comparison with the axis of greatest multivariate divergence, Cline_{max} (from Stock et al. 2014). In Cline_{max} both corolla width and anther-stigma distance showed significant among-population divergence of the means, which suggests that the paucity of within-population variation for these traits is due to selection.

Our analysis of the geometric similarity of **G** through Krzanowski's subspace analysis showed that the majority of within-population genetic (co)variation of our populations share overlapping trait space. Our results are suggestive of the overall stability of the **G** matrices across populations, with no evidence of differences between range-edge and core populations in the trait space where most (co)variation lies. In this regard, our results are similar to McGoey and Stinchcombe (2021), who found little difference in **G** matrices between introduced and native populations of ragweed (*Ambrosia artemisiifolia*) despite expectations to the contrary. More generally, our results add to other findings of **G** being relatively stable across geography (Arnold et al. 2008; Delahaie et al. 2017). Work on the cuticular hydrocarbons of *Drosophila serrata* population by Hine and colleagues (Hine et al 2009, Chenoweth et al. 2008) did find patterns in mean trait divergence, reduction in associated variation in g_{max}, and divergence among populations along g_{max}. Similarly, Aguirre et al (2014) found that the populations share considerable trait space, although there were axes of divergence among the populations.

The independently estimated sexual selection gradient is nearly orthogonal with respect to g_{max}, however, and thus the mostly likely explanation for the majority of the divergence among these populations was drift (Hine et al 2009).

Both the covariance tensor and random skewers analysis suggest that the Hoffman, NC population differed from the others (this population also had the most genetic variation overall, the highest effective number of dimensions, and the most genetic variance in the direction of clinal divergence). The covariance tensor and skewers approaches are complementary, in that the tensor reflects patterns of variation and covariation among G, while the skewers analysis is not sensitive to differences in the total amount of genetic variance and magnitude of the response (as it uses the correlation between response vectors, but not their magnitude; Hansen and Houle 2008) and so these differences are not only due to Hoffman's greater overall genetic variation. The first eigenvector of the first eigentensor (*e11*), the first eigenvector of the random skewers analysis (*RSe1*), and g_{max} within the Hoffman population were all highly correlated, with heavy loading from flowering time, corolla width, and seed mass. While the greater overall genetic variation in Hoffman may not have directly led to these differences between matrices, it may have allowed Hoffman greater evolvability, allowing for an increase in observable differences when compared to the other populations. The Hoffman, NC population site did not differ substantially from the others: all were collected from roadsides adjacent to agricultural fields, and were reasonably large to allow for sampling from 70-100 individuals. Hoffman was, however, the only population where we observed both leaf shape genotypes (leaf shape is a simple Mendelian polymorphism in this species; Bright 1998). Some speculative possibilities are that it was founded by heterozygous individuals, multiple founders of opposite leaf shape

genotypes, or is subject to balancing selection on the leaf shape locus (as has been shown by Bright and Rausher 2008), and thus has more variation for these reasons.

Collectively, our diverse set of analyses points to a single population being qualitatively different from the others, with divergence driven by a handful of traits in that population, rather than range-edge populations having any inherent differences in the structure of **G**. At face value, these findings might suggest that range-edge populations are not small enough to experience substantial genetic drift that could reduce genetic variance compared to central populations; alternatively, it may be that all populations experience frequent extinction and colonization dynamics, across the range, and that this does not have differential effects on genetic variance. We suspect the latter possibility is more likely.

Clinal divergence and G

In general, phenotypic divergence is expected to be aligned with **G** under three overall conditions. First, under genetic drift, we expect that phenotypic divergence in a suite of traits should be related to the overall amount of standing quantitative genetic variance in those traits (Lande 1979, Phillips et al. 2001). Second, when **G** matrices are ill-conditioned, or of reduced rank, we expect evolutionary responses to be biased towards the directions of multivariate trait space with genetic variance (Chenoweth et al. 2010). In other words, once a **G** matrix differs from spherical, evolutionary responses will be dominated by the directions containing the most variance. Finally, when $\beta = g_{max}$, we expect the maximal evolutionary response, and a concordance between Δz, g_{max}, and β (Gaydos et al. 2013). Hangartner et al. (2019) found that the **G** matrices of range edge populations of *Drosophila melanogaster* were in fact aligned with the axis of clinal divergence and that the trait covariances improved the adaptive potential of peripheral populations. In contrast, phenotypic divergence does not have to be aligned with **G** if

selection has been strong and persistently favoring alternative combinations of traits. For example, McGuigan et al. (2005), found that the direction of hydrodynamic adaptation in rainbow fish was only weakly associated with g_{max}, and was primarily aligned with the trailing eigenvectors of **G**; they interpreted this as a result of long-term selection towards a new phenotypic optimum.

With this context in mind, many of our results suggest that we should have observed a relationship between clinal divergence and **G**: the traits are genetically variable, both individually (Table S1) and as a linear combination (Table 2), and the **G** matrices appear to be ill-conditioned and of low effective number of dimensions (Table 1). It also seems unlikely that the phenotypic divergence detected is a result of long-term selection, similar to McGuigan et al. (2005), as *I. hederacea* currently inhabits (and was collected from) ephemeral, disturbance-prone habitats such as roadsides, agricultural fields, and cleared areas. Consequently, many of the conditions that can produce a relationship between **G** and divergence appear to be met.

Two potential explanations for why we do not see such a relationship between **G** and divergence occur to us. The first is that our previous work (Simonsen and Stinchcombe 2010; Campitelli and Stinchcombe 2013; Stock et al. 2014) and this study inadvertently omitted an ecologically important, correlated trait. For this scenario to explain the lack of relationship between divergence and **G**, there would have to be an omitted trait that is both highly variable within populations, and highly diverged between populations, such that its inclusion would predominate both g_{max} and any estimate of a divergence vector. The problem of missing traits is inherent to studies of phenotypic evolution; while the traits we measured capture aspects of size, growth, phenology, and floral morphology, it is possible that other traits related to ecophysiology, seed bank dynamics, or other aspects of the life cycle are more important.

Second, it may be the case that natural selection is acting in a direction that is nearly orthogonal to g_{max}, thus leading to the divergence that is at a substantial angle from g_{max}. If this were the case, it would be possible for the **G** matrices we estimated to produce evolutionary responses that could lead to the observed divergence. One clue in support of this hypothesis is that flowering time appears to load relatively weakly on g_{max} in the Pennsylvania population, but in the past has been detected to be under very strong directional selection in this species (Simonsen and Stinchcombe 2010; Campitelli and Stinchcombe 2013). Similarly, Campitelli and Stinchcombe (2013) found selection favoring decreased flowering time and increased early and mid-season growth rates (i.e., β elements of opposite signs), while we found that growth rate and flowering time load in the same direction (i.e., are positively correlated) of g_{max} in three of four populations. As such, there are past observations of selection acting strongly on traits with relatively little genetic variance, or in opposite directions on positively correlated traits, both of which could lead to β being orthogonal to g_{max}. Indeed, Simonsen and Stinchcombe (2010) found strong natural selection almost orthogonal to g_{max} in a field study of size traits and flowering time, due to size traits being highly variable and under weak selection, and flowering time being less variable but under very strong selection. The divergence observed may thus be the product of selection, but without requiring recourse to long-term selection towards a single optimum. While there are field studies of natural selection on some of the traits we studied, an overall study of all of them is necessary to distinguish between the missing trait explanation and β being orthogonal to g_{max}.

Conclusions and Future Directions

Determining the relationship between **G** and phenotypic divergence, or divergence of **G** matrices themselves, is a challenging empirical and statistical endeavor. Practical constraints

make constructing well estimated **G** matrices for dozens of populations nearly impossible (Arnold et al. 2008), and is certainly the case for *I. hederacea*. The most tractable and testable hypothesis to emerge from our work is that natural selection on these five traits is poorly aligned with g_{max}. Future field studies will be required to further elucidate the action of natural selection on this species, and the ecological mechanisms behind selection for this suite of traits and others.

Acknowledgments

We thank NSERC Canada for funding and a Koffler Scientific Reserve graduate fellowship (GH) for support. We thank Tia Harrison for field assistance, Brechann McGoey for sharing relevant R scripts and advice, Jacqueline Sztepanacz for comments on the manuscript, and Aneil Agrawal, Asher Cutter, Matt Osmond, and Stephen Wright for discussion. Greenhouse support from William Cole, Tom Gludovacz, Colin Bonner, and Andrew Petrie was invaluable.

References

Agrawal, A. F., and J. R. Stinchcombe. 2009. How much do genetic covariances alter the rate of adaptation? Proc. Biol. Sci. 276:1183–1191.

Aguirre, J. D., E. Hine, K. McGuigan, and M. W. Blows. 2014. Comparing G: multivariate analysis of genetic variation in multiple populations. Heredity 112:21–29.

Antonovics, J. 1976. The Nature of Limits to Natural Selection. Ann. Mo. Bot. Gard. 63:224–247. Missouri Botanical Garden Press.

Arnold, S. J., R. Bürger, P. A. Hohenlohe, B. C. Ajie, and A. G. Jones. 2008. Understanding the evolution and stability of the G-matrix. Evolution 62:2451–2461.

Basser, P. J., and S. Pajevic. 2007. Spectral decomposition of a 4th-order covariance tensor: Applications to diffusion tensor MRI. Signal Processing 87:220–236.

Bright-Emlen, K. L. 1998. Geographic variation and natural selection on a leaf shape polymorphism in the ivyleaf morning glory (*Ipomoea hederacea*). Duke University, Ann Arbor, United States.

Bright, K. L., and M. D. Rausher. 2008. Natural selection on a leaf-shape polymorphism in the ivyleaf morning glory (*Ipomoea hederacea*). Evolution 62:1978–1990.

Brown, J. H., D. W. Mehlman, and G. C. Stevens. 1995. Spatial variation in abundance. Ecology 76:2028–2043.

Campitelli, B. E., and J. R. Stinchcombe. 2013. Natural selection maintains a single-locus leaf shape cline in Ivyleaf morning glory, *Ipomoea hederacea*. Mol. Ecol. 22:552–564.

Campitelli, B. E., and J. R. Stinchcombe. 2014. Population dynamics and evolutionary history of the weedy vine *Ipomoea hederacea* in North America. G3 4:1407–1416.

Chenoweth, S. F., H. D. Rundle, and M. W. Blows. 2008. Genetic constraints and the evolution of display trait sexual dimorphism by natural and sexual selection. Am. Nat. 171:22–34.

Chenoweth, S. F., H. D. Rundle, and M. W. Blows. 2010. The contribution of selection and genetic constraints to phenotypic divergence. Am. Nat. 175:186–196.

Cheverud, J. M., and G. Marroig. 2007. Comparing covariance matrices: Random skewers method compared to the common principal components model. Genetics and Molecular Biology 30:461–469.

Delahaie, B., A. Charmantier, S. Chantepie, D. Garant, M. Porlier, and C. Teplitsky. 2017. Conserved G-matrices of morphological and life-history traits among continental and island blue tit populations. Heredity 119:76–87.

Endler, J. A. 1977. Geographic Variation, Speciation and Clines. Princeton University Press.

Ennos, R. A. 1981. Quantitative studies of the mating system in two sympatric species of *Ipomoea* (Convolvulaceae). Genetica 57:93–98.

Falconer, D. S., and T. F. C. Mackay. 1996. Introduction to quantitative genetics. Fourth. Essex, UK: Longman Group.

Garcia-Ramos, G., and M. Kirkpatrick. 1997. Genetic models of adaptation and gene flow in peripheral populations.

Gaydos, T. L., N. E. Heckman, M. Kirkpatrick, J. R. Stinchcombe, J. Schmitt, J. Kingsolver, and J. S. Marron. 2013. Visualizing genetic constraints. Ann. Appl. Stat. 7:860–882.

Guillaume, F., and M. C. Whitlock. 2007. Effects of migration on the genetic covariance matrix. Evolution 61:2398–2409.

Hadfield, J. D. 2010. MCMC Methods for Multi-Response Generalized Linear Mixed Models: The MCMCglmm R Package. J. Stat. Softw. 33:1–22.

Hangartner, S., Lasne, C., Sgrò C.M., Connallon T., and K. Monro. 2019. Genetic covariances promote climatic adaptation in Australian *Drosophila*. Evolution 74: 326-337.

Hansen, T. F., and D. Houle. 2008. Measuring and comparing evolvability and constraint in multivariate characters. J. Evol. Biol. 21:1201–1219.

Hine, E., S. F. Chenoweth, H. D. Rundle, and M. W. Blows. 2009. Characterizing the evolution of genetic variance using genetic covariance tensors. Philos. Trans. R. Soc. Lond. B Biol. Sci. 364:1567–1578.

Hull-Sanders, H. M., M. D. Eubanks, and D. E. Carr. 2005. Inbreeding depression and selfing rate of *Ipomoea hederacea* var. *integriuscula* (Convolvulaceae). Am. J. Bot. 92:1871–1877.

Jones, A. G., S. J. Arnold, and R. Bürger. 2004. Evolution and stability of the G-matrix on a landscape with a moving optimum. Evolution 58:1639–1654.

Kingsolver, J. G., N. Heckman, J. Zhang, P. A. Carter, J. L. Knies, J. R. Stinchcombe, and K. Meyer. 2015. Genetic variation, simplicity, and evolutionary constraints for function-valued traits. Am. Nat. 185:E166–81.

Kirkpatrick, M. 2009. Patterns of quantitative genetic variation in multiple dimensions. Genetica 136:271–284.

Kirkpatrick, M., and N. H. Barton. 1997. Evolution of a species' range. Am. Nat. 150:1–23.

Klingaman, T. E., and L. R. Oliver. 1996. Existence of ecotypes among populations of entireleaf morningglory (*Ipomoea hederacea* var. *integriuscula*). Weed Sci. 44:540–544.

Krzanowski, W. J. 1979. Between-groups comparison of principal components. J. Am. Stat. Assoc. 74:703–707.

Lande, R. 1992. Neutral theory of quantitative genetic variance in an island model with local extinction and colonization. Evolution 46:381–389.

Lande, R. 1979. Quantitative genetic analysis of multivariate evolution, applied to brain: body size allometry. Evolution 33:402–416.

Lande, R., and S. J. Arnold. 1983. The measurement of selection on correlated characters. Evolution 37:1210–1226.

Lin, C. Y., and F. R. Allaire. 1977. Heritability of a linear combination of traits. Theor. Appl. Genet. 51:1–3.

Mayr, E. 1963. Animal Species and Evolution. Harvard University Press.

Mayr, E. 1954. Change of genetic environment and evolution. George Allen & Unwin Limited.

McGoey, B. V., and J. R. Stinchcombe. 2021. Introduced populations of ragweed show as much evolutionary potential as native populations. Evol. Appl. 14:1436–1449.

McGuigan, K., S. F. Chenoweth, and M. W. Blows. 2005. Phenotypic divergence along lines of genetic variance. Am. Nat. 165:32–43.

Morrissey, M. B., S. Hangartner, and K. Monro. 2019. A note on simulating null distributions for G matrix comparisons. Evolution 73:2512–2517.

Peterson, R. A., and J. E. Cavanaugh. 2020. Ordered quantile normalization: a semiparametric transformation built for the cross-validation era. J. Appl. Stat. 47:2312–2327.

Phillips, P. C., M. C. Whitlock, and K. Fowler. 2001. Inbreeding changes the shape of the genetic covariance matrix in *Drosophila melanogaste*r. Genetics 158:1137–1145.

Puentes, A., G. Granath, and J. Ågren. 2016. Similarity in G matrix structure among natural populations of *Arabidopsis lyrata*. Evolution 70:2370–2386.

Roff, D. 2000. The evolution of the G matrix: selection or drift? Heredity 84:135–142.

Roughgarden, J. 1979. Theory of population genetics and evolutionary ecology : an introduction. Macmillan, New York.

Sexton, J. P., P. J. McIntyre, A. L. Angert, and K. J. Rice. 2009. Evolution and ecology of species range limits. Annu. Rev. Ecol. Evol. Syst. 40:415–436. Annual Reviews.

Simonsen, A. K., and J. R. Stinchcombe. 2010. Quantifying evolutionary genetic constraints in the ivyleaf morning glory, *ipomoea hederacea*. Int. J. Plant Sci. 171:972–986.

Stock, A. J., B. E. Campitelli, and J. R. Stinchcombe. 2014. Quantitative genetic variance and multivariate clines in the Ivyleaf morning glory, *Ipomoea hederacea*. Philos. Trans. R. Soc. Lond. B Biol. Sci. 369:20130259.

Sztepanacz, J. L., and M. W. Blows. 2017. Accounting for Sampling Error in Genetic Eigenvalues Using Random Matrix Theory. Genetics 206:1271–1284.

Teplitsky, C., M. R. Robinson, and J. Merilä. 2014. Evolutionary potential and constraints in wild populations. Quantitative genetics in the wild 190–208. Oxford University Press Oxford, UK.

Walsh, B., and M. W. Blows. 2009. Abundant genetic variation + strong selection = multivariate genetic constraints: a geometric view of adaptation. Annu. Rev. Ecol. Evol. Syst. 40:41–59.

Walter, G. M., J. David Aguirre, M. W. Blows, and D. Ortiz-Barrientos. 2018. Evolution of genetic variance during adaptive radiation. Am. Nat. 191:E108–E128.

Whitlock, M. C., and D. E. McCauley. 1990. Some population genetic consequences of colony formation and extinction: genetic correlations within founding groups. Evolution 44:1717–1724.

Wood, C. W., and E. D. Brodie 3rd. 2015. Environmental effects on the structure of the G-matrix. Evolution 69:2927–2940.